

Article

Synthesis and Properties of 2-Alkylidene-1,3-dithiolo[4,5-*d*]-4,5-ethylenediselenotetrathiafulvalene Derivatives and Crystal Structures of Their Cation Radical Salts

Keisuke Furuta, Shuhei Kohno, Takashi Shirahata *, Koya Yamasaki, Shojun Hino and Yohji Misaki

Department of Applied Chemistry, Graduate School of Science and Engineering, Ehime University, 3 Bunkyo-cho, Matsuyama 790-8577, Japan; E-Mails: furuta.redg@gmail.com (K.F.); shushu850@gmail.com (S.K.); yamasaki.koya.ts@gmail.com (K.Y.); hino.shojun.mk@ehime-u.ac.jp (S.H.); misaki.yohji.mx@ehime-u.ac.jp (Y.M.)

* Author to whom correspondence should be addressed; E-Mail: shirahata.takashi.mj@ehime-u.ac.jp; Tel.: +81-89-927-8537; Fax: +81-89-927-9922.

Received: 23 March 2012; in revised form: 24 April 2012 / Accepted: 24 April 2012 /

Published: 9 May 2012

Abstract: Tetrathiafulvalene derivatives condensed with 2-alkylidene-1,3-dithiole moiety, MeDTES (2-isopropylidene-1,3-dithiolo[4,5-*d*]-4,5-ethylenediselenotetrathiafulvalene), EtDTES (2-(pentan-3-ylidene)-1,3-dithiolo[4,5-*d*]-4,5-ethylenediselenotetrathiafulvalene), and CPDTES (2-cyclopentanylidene-1,3-dithiolo[4,5-*d*]-4,5-ethylenediselenotetrathiafulvalene) have been synthesized. Crystal structure analysis of MeDTES salts with $\text{Au}(\text{CN})_4^-$, ReO_4^- , and I_3^- and a CPDTES salt with I_3^- reveals that the donor–anion ratios of all salts are 1:1. Band calculation of $(\text{MeDTES})[\text{Au}(\text{CN})_4]$ suggests a quasi-one-dimensional Fermi surface that could be the result of the uniform stack of donor molecules. In spite of this stacking, the salt is a Mott insulator because of a large on-site Coulomb interaction U . $(\text{MeDTES})(\text{ReO}_4)(\text{H}_2\text{O})_{0.5}$ possesses Fermi points and exhibits semiconducting behavior with small activation energy ($E_a = 0.058$ eV). I_3^- ions form disordered infinite chain in $(\text{MeDTES})(\text{I}_3)(\text{DCE})_{0.25}$, but those in $(\text{CPDTES})(\text{I}_3)$ exist as discrete ions. They show low conductivity (10^{-4} – 10^{-2} S cm^{-1}) at room temperature and the band calculation suggests that they are band insulator.

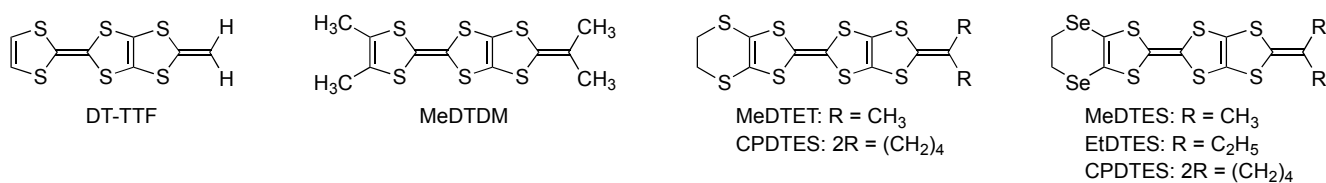
Keywords: molecular conductors; tetrathiafulvalene derivatives; cation radical salts; crystal structure; band calculation

1. Introduction

Two-dimensional organic superconductors based on bis(ethylenedithio)tetrathiafulvalene (BEDT-TTF) have been developed and some of them have showed a superconducting transition above 10 K [1–4]. Two-dimensional molecular arrangements such as β - and κ -types [5,6] and the effective half filled band are important to produce high T_c organic superconductors. In the β - and κ -types, donor molecules form face-to-face dimers, and they form two-dimensional conducting layers. Introduction of appropriate substituents introducing steric hindrance is regarded as an effective strategy to obtain a dimerized molecular arrangement. Actually, a large number of TTF derivatives have been synthesized in order to develop novel molecular conductors with a two-dimensional molecular arrangement. TTF derivatives condensed with 2-alkylidene-1,3-dithiole moiety (DT-TTFs) containing methyl groups or an ethylenedithio group, 2-isopropylidene-1,3-dithiolo[4,5-*d*]-4,5-dimethyltetrathiafulvalene (MeDTDM), 2-isopropylidene-1,3-dithiolo[4,5-*d*]-4,5-ethylenedithiotetrathiafulvalene (MeDTET), and 2-cyclopentanylidene-1,3-dithiolo[4,5-*d*]-4,5-ethylenedithiotetrathiafulvalene (CPDTET), often provide such salts possessing the two-dimensional β - and κ -type molecular arrangements that show metallic conductivity down to low temperature. They did not, however, show superconductivity because their metallic nature derived from a wide bandwidth is too stable [7,8] and the non-half-filled band, such as the quarter-filled band [9], the 5/6 filled band with 3:1 composition [10], and the non-stoichiometric band filling [11].

To reduce bandwidth of the molecular conductors based on MeDTET and CPDTET, we designed new electron donors, 2-isopropylidene-1,3-dithiolo[4,5-*d*]-4,5-ethylenediselenotetrathiafulvalene (MeDTES), 2-(pentan-3-ylidene)-1,3-dithiolo[4,5-*d*]-4,5-ethylenediselenotetrathiafulvalene (EtDTES), and 2-cyclopentanylidene-1,3-dithiolo[4,5-*d*]-4,5-ethylenediselenotetrathiafulvalene (CPDTES) as depicted in Figure 1. Replacement of sulfur atoms by selenium atoms on the π -system usually extends the bandwidth [12–14]. In contrast, introduction of substituents containing selenium atoms reduces the intermolecular interaction because of their steric hindrance and selenium atoms have small coefficients in the highest occupied molecular orbital (HOMO) [15,16]. Introduction of the ethylenediseleno group in the DT-TTF derivatives could bring the reduction of the bandwidth of the system, which might be helpful to develop new superconductors. Here we report the synthesis and properties of MeDTES, EtDTES, and CPDTES together with structures of their cation radical salts.

Figure 1. Molecular structures of TTF derivatives condensed with 2-alkylidene-1,3-dithiole unit (DT-TTFs).



2. Results and Discussion

2.1. Synthesis and Property of MeDTES, EtDTES, and CPDTES

The synthesis of MeDTES, EtDTES, and CPDTES is outlined in Figure 2. The triethyl phosphite-mediated cross-coupling reaction of 4,5-ethylenediseleno-1,3-dithiole-2-thione (**1**) [17] with the ketone **2** [18] afforded phosphonate ester **3** in a 62% yield [19]. MeDTES, EtDTES and CPDTES were synthesized in a 68–86% yield by the Wittig–Horner reaction of **3** with corresponding ketone in the presence of lithium diisopropylamide (LDA) in THF at $-78\text{ }^{\circ}\text{C}$. Molecular structures of all the new compounds were determined by NMR, MS, and elemental analyses. Redox potentials were measured by cyclic voltammetry (CV) in benzonitrile. The cyclic voltammograms of MeDTES, EtDTES, and CPDTES showed two pairs of reversible redox waves and one pair of irreversible waves. The redox potentials are summarized in Table 1. The first oxidation potentials of these donors are lower by 0.01–0.02 V than those of MeDTET and BEDT-TTF [20], which could be due to the smaller electronegativity of the selenium atom compared with that of the sulfur atom. There is not, however, much difference in the electron-donating ability between these new donors and MeDTET.

Figure 2. Synthesis of MeDTES, EtDTES, and CPDTES.

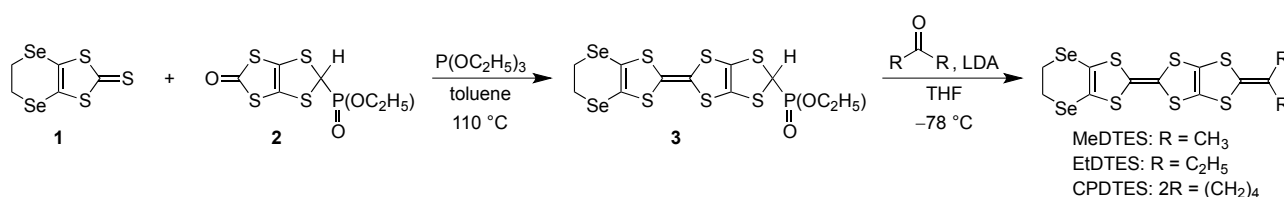


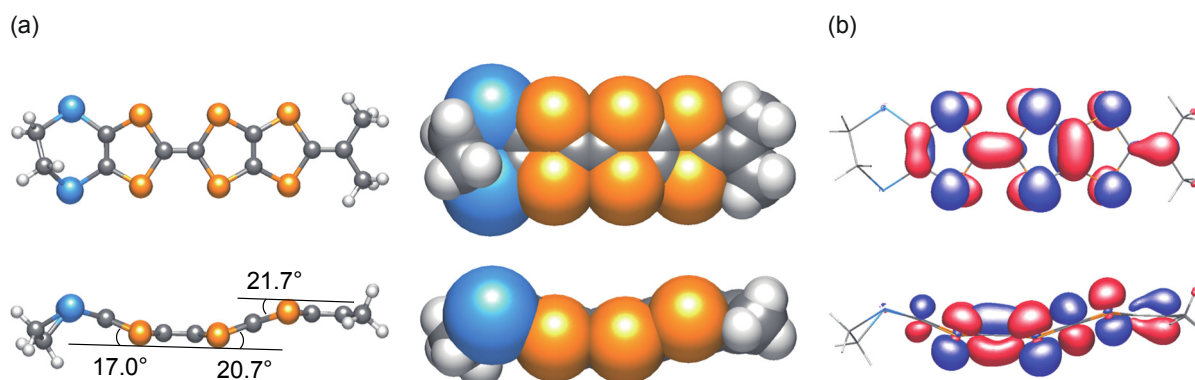
Table 1. Redox potentials ^a (V vs. Fc/Fc⁺) of MeDTES, EtDTES, CPDTES, and related compounds.

Donor	E_1	E_2	E_3^b	$\Delta E (=E_2 - E_1)$
MeDTES	0.04	0.34	1.00	0.30
EtDTES	0.05	0.35	1.01	0.30
CPDTES	0.04	0.35	1.00	0.31
MeDTET	0.06	0.37	0.99	0.31
BEDT-TTF ^c	0.06	0.38	—	0.32

^a Measured in benzonitrile containing 0.1 M ⁿBu₄NPF₆, scan rate was 50 mV s⁻¹; ^b Irreversible wave. Anodic peak potentials; ^c Measured in benzonitrile containing 0.1 M ⁿBu₄NBF₄, scan rate was 100 mV s⁻¹ [20].

The theoretical calculation of MeDTES was carried out using a hybrid method of Hartree-Fock and density functional theory (DFT) B3LYP methods using the 6–31G(d) basis set. Figure 3 shows an optimized structure and the HOMO of MeDTES. The TTF moiety adopts a chair conformation and the dihedral angles are 17.0 and 20.7°. The 2-isopropylpyridine-1,3-dithiole unit also bends with the dihedral angle of 21.7°. The terminal six-membered ring of MeDTES has an eclipsed conformation [15] and the selenium atoms of the ethylenediseleno group protrude from the DT-TTF skeleton, that is, the ethylenediseleno group is so bulky that is a crucial factor to form a dimer structure. The HOMO of MeDTES distributes mainly to the DT-TTF moiety and hardly distributes to the ethylenediseleno group.

Figure 3. (a) Top view and side view of optimized structure of MeDTES are represented by a ball and stick model (left) and a space-filling model (right); (b) The HOMO of MeDTES, of which the energy level is -4.72 eV.



2.2. Preparation, Structures of Cation Radical Salts

2.2.1. Preparation of Cation Radical Salts

Single crystals of the cation radical salts of MeDTES and CPDTES were prepared by electrocrystallization in tetrahydrofuran, 1,2-dichloroethane (containing 6% ethanol, *v/v*), and chlorobenzene (containing 6% ethanol, *v/v*) in the presence of corresponding tetra-*n*-butylammonium salts as the supporting electrolyte (Table 2). The salts of MeDTES with $\text{Au}(\text{CN})_4^-$ (**4**), ReO_4^- (**5**), and I_3^- (**6**) and the CPDTES salt with I_3^- (**7**) were obtained as platelet crystals, although EtDTES did not afford single crystalline salts. Crystal data of **5–7** are summarized in Table 3.

Table 2. Conditions of the preparation of **4–7**^a.

Salt	Donor (/ mg)	Electrolyte (/ mg) ^b	Solvent, 18 mL ^c	Current/ μA	Period/day
4	MeDTES (2.0)	TBAAu(CN) ₄ (39.1)	THF	0.5	2
5	MeDTES (2.0)	TBAReO ₄ (35.5)	THF	0.5	2
6	MeDTES (2.0)	TBAI ₃ (44.9)	DCE (6% EtOH)	0.5	2
7	CPDTES (2.0)	TBAI ₃ (44.9)	PhCl (6% EtOH)	0.5	2

^a 25 °C under an argon atmosphere; ^b The tetra-*n*-butylammonium (TBA) salts were employed;

^c THF = tetrahydrofuran; DCE = 1,2-dichloroethane; PhCl = chlorobenzene; EtOH = ethanol.

Table 3. Crystal data, structure refinement details and electrical properties for **4–7**.

Compound	4	5	6	7
CCDC no.	879812	879813	879814	879815
Chemical formula	$\text{C}_{12}\text{H}_{10}\text{S}_6\text{Se}_2 \cdot \text{AuC}_4\text{N}_4$	$\text{C}_{12}\text{H}_{10}\text{S}_6\text{Se}_2 \cdot \text{ReO}_4 \cdot (\text{H}_2\text{O})_{0.5}$	$(\text{C}_{12}\text{H}_{10}\text{S}_6\text{Se}_2)_2 \cdot (\text{I}_6) \cdot (\text{C}_4\text{H}_4\text{Cl}_2)_{0.5}$	$\text{C}_{14}\text{H}_{12}\text{S}_6\text{Se}_2 \cdot \text{I}_3$
Formula weight	805.53	763.69	1819.84	911.22
Crystal size (mm^3)	$0.05 \times 0.04 \times 0.01$	$0.04 \times 0.02 \times 0.01$	$0.06 \times 0.02 \times 0.01$	$0.08 \times 0.06 \times 0.03$
Crystal system	Orthorhombic	Triclinic	Triclinic	Triclinic

Table 3. Cont.

Compound	4	5	6	7
Space group	<i>Pnma</i>	<i>P1</i>	<i>P1</i>	<i>P1</i>
<i>a</i> /Å	42.054(4)	8.532(6)	7.893(2)	8.443(2)
<i>b</i> /Å	12.3735(9)	9.750(7)	8.594(3)	8.859(2)
<i>c</i> /Å	4.2760(3)	13.597(10)	34.646(10)	16.686(5)
α /°	90	94.949(17)	89.481(8)	84.118(11)
β /°	90	94.723(14)	84.178(6)	89.712(13)
γ /°	90	93.783(13)	77.788(4)	68.365(9)
<i>V</i> /Å ³	2225.0(3)	1120.0(14)	2285.0(12)	1153.2(5)
<i>Z</i>	4	2	2	2
<i>D</i> _{calc} /mg m ⁻³	2.405	2.264	2.645	2.624
μ /mm ⁻¹	10.459	9.250	7.894	7.764
Temperature/K	273	120	273	273
Measured reflections	19893	13612	23602	9519
Independent reflections (<i>R</i> _{int})	2660 (0.0660)	5066 (0.0800)	10260 (0.0856)	5193 (0.0705)
Observed reflections [<i>I</i> ≥ 2σ(<i>I</i>)]	2464	3763	6592	2485
Restraints/parameters	0/149	0/206	0/437	0/229
<i>R</i> ₁ / <i>wR</i> ₂ [<i>I</i> ≥ 2σ(<i>I</i>)]	0.0535, 0.1123	0.0835, 0.2044	0.0654, 0.1591	0.0455, 0.0993
<i>R</i> ₁ / <i>wR</i> ₂ (all data)	0.0593, 0.1154	0.1084, 0.2303	0.1006, 0.1818	0.0972, 0.1235
Goodness of fit	1.214	1.070	1.093	0.902
σ_{rt} /S cm ⁻¹	4.4 × 10 ⁻³	1.3 × 10 ⁻²	5.3 × 10 ⁻²	6.1 × 10 ⁻⁴
<i>E</i> _a /eV	0.15	0.058	0.051	0.17

2.2.2. Structures and Electrical Properties of (MeDTES)[Au(CN)₄] (4)

(MeDTES)[Au(CN)₄] (4) crystallizes in orthorhombic space group *Pnma*. The ORTEP drawings of the MeDTES molecule are shown in Figure 4. A half of the donor molecule is crystallographically independent, in which the carbon atoms C3, C4, C6, and C7 are on the mirror plane at *b* = 0.25. The terminal ethylene bridge of the MeDTES molecule shows a flipping disorder. The gold atom of the Au(CN)₄⁻ ion also exists on the mirror plane at *b* = 0.75 and half of the Au(CN)₄⁻ ion is crystallographically independent. These facts indicate a 1:1 donor–anion ratio. Donor molecules stack uniformly along the *c* axis with the interplanar distance *z* = 3.49 Å and the slipping distance *x* = 2.47 Å in a head-to-head manner. The geometrical parameters *x*, *y*, and *z* are estimated by the literature method [5], and the definition of these parameters is shown in Supplementary Materials. There are four, crystallographically equivalent donor columns in the unit cell: I, II, III, and IV (Figure 5). The Se⋯Se contact (3.720(1) Å) is shorter than the sum of the van der Waals radii [21], which are represented by blue broken lines in Figure 5. The adjacent donor columns I and II (III and IV) are orthogonally linked by the Se⋯Se contacts along the *b* axis. The square-planar Au(CN)₄⁻ ions also stack along the *c* axis with the interplanar distance of 3.24 Å. In consequence, this salt shows a segregate columnar structure like (TTF)(TCNQ) [22].

Figure 4. Top view (left) and side view (right) of ORTEP drawings of the MeDTES molecule in **4**. Displacement ellipsoids are drawn at the 50% probability level. Symmetry operator * is $x, 0.5 - y, z$.

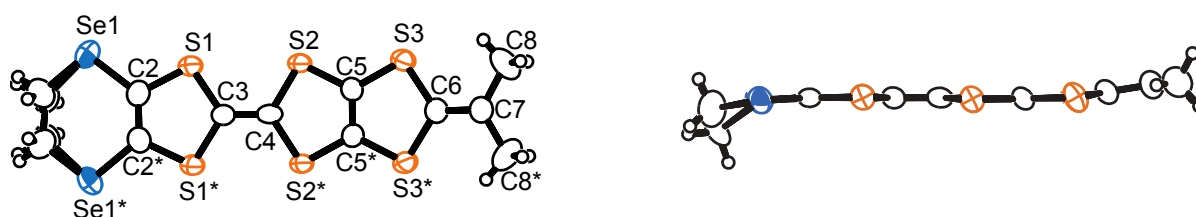
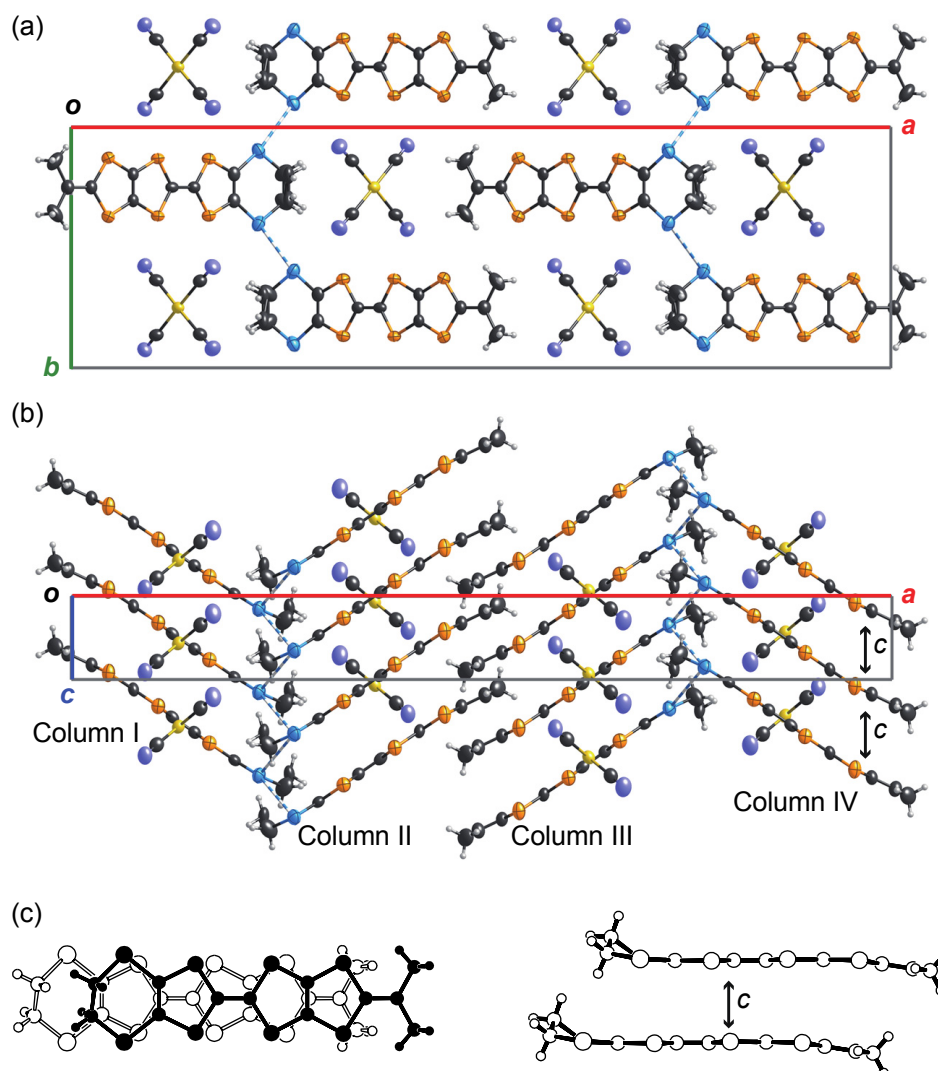


Figure 5. Crystal structures of **4** (a) viewed along the c axis and (b) b axis. Blue broken lines indicate the $\text{Se}\cdots\text{Se}$ contacts, shorter than the sum of the van der Waals radii; (c) Top view and side view of molecular overlap of c . The atoms in the front molecule are represented by solid circles and those in the rear are represented by open circles. One of the conformations for the ethylene bridge is omitted for clarity.



Intermolecular overlap integrals are calculated by the extended Hückel method [23] and are listed in Figure 6. Intrastack overlap integral c (-26.80×10^{-3}) is much larger than integrals $b1$, $b2$, and p . The calculated band dispersion and the Fermi surfaces for **4** based on the tight-binding approximation are

shown in Figure 7 [23]. The energy band shows a half-filled band because of the 1:1 donor–anion ratio and uniform donor column. The flat Fermi surfaces suggest that this salt is a one-dimensional metal. This salt shows, however, low conductivity ($\sigma_{rt} = 4.4 \times 10^{-3} \text{ S cm}^{-1}$) at room temperature and semiconducting behavior with an activation energy of $E_a = 0.15 \text{ eV}$. The redox potential difference, ($\Delta E = E_2 - E_1$), corresponds to the on-site Coulomb interaction U . The ΔE value of MeDTES (0.30 V) is almost the same as that of BEDT-TTF (0.32 V [20]). These facts suggest that this salt is a Mott insulator derived from the relatively large on-site Coulomb interaction U .

Figure 6. Molecular arrangements of (a) columns I and II viewed along the molecular short axis and (b) columns II and III viewed along the molecular long axis. The calculated overlap integrals ($\times 10^{-3}$) are $c = -26.80$, $b1 = 0.20$, $b2 = -0.02$, and $p = -0.58$. The hydrogen atoms are omitted for clarity.

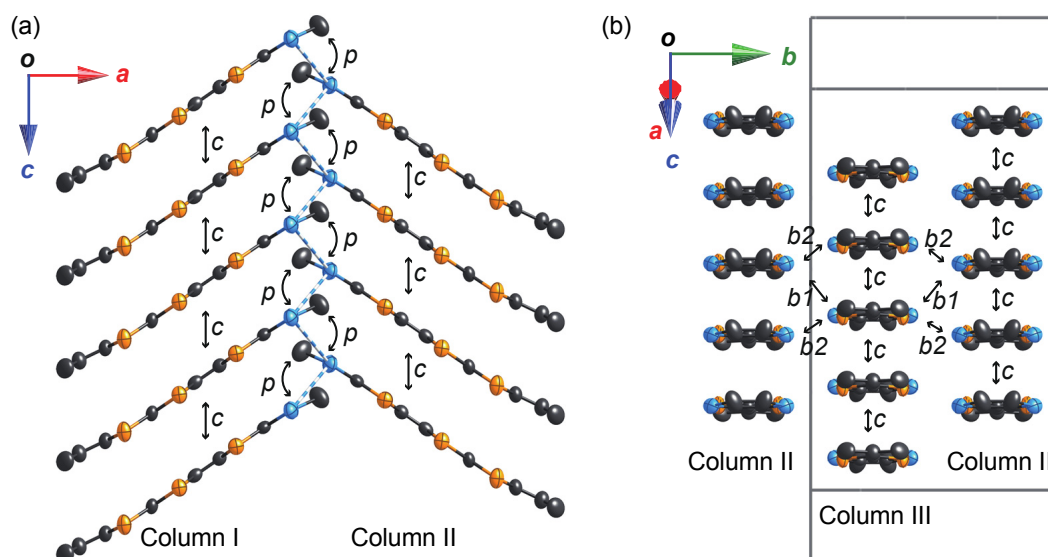
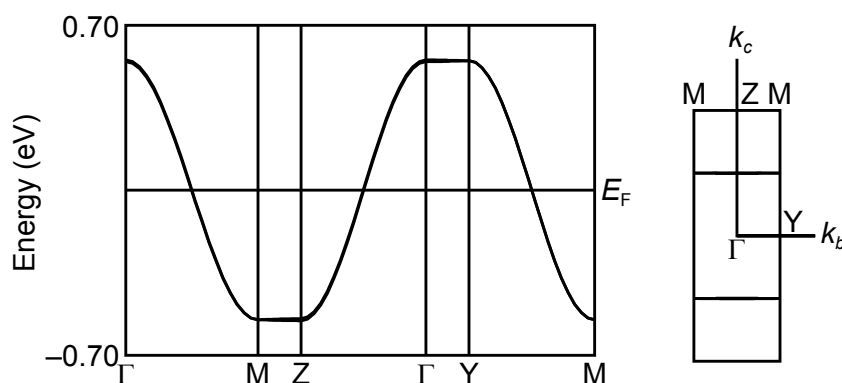


Figure 7. Calculated band dispersion (left) and Fermi surfaces (right) for 4.

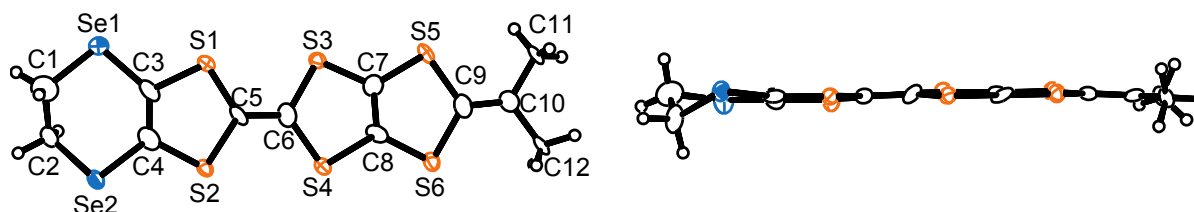


2.2.3. Structures and Electrical Properties of (MeDTES)(ReO₄)(H₂O)_{0.5} (5)

(MeDTES)(ReO₄)(H₂O)_{0.5} (5) crystallizes in triclinic space group $P\bar{1}$. The molecular structure of the donor molecule is shown in Figure 8. The MeDTES molecule in this salt shows high planarity except for the terminal ethylene bridge. One donor molecule and one ReO₄[−] ion are crystallographically independent and they are located in the general position, giving the 1:1 donor–anion ratio. An oxygen

atom is found around the center of inversion with a half occupancy. Since the origin of the oxygen is not clear, we assumed it as a part of the solvent, tetrahydrofuran (THF). However, the refinement did not converge to give the THF molecule. Therefore we conclude that the oxygen atom is either water (H_2O) or of oxonium ion (H_3O^+) origin, which might explain the conducting property of the salt.

Figure 8. Top view (left) and side view (right) of ORTEP drawings of the MeDTES molecule in **5**. Displacement ellipsoids are drawn at the 50% probability level.



As shown in Figure 9, donor molecules form a columnar structure along the a axis and they are linked by $\text{Se}\cdots\text{S}$ contact ($3.682(5)$ Å) which is shorter than the sum of the van der Waals radii ($\text{Se}\cdots\text{S} = 3.70$ Å) [21]. The donor molecules stack in a two-fold periodicity with the interplanar distance of 3.65 Å for a_1 and 3.33 Å for a_2 . The slipping distance x along the molecular long axis is 9.01 Å for a_1 and 4.60 Å for a_2 [5]. The donor molecules are also slipping by 1.97 Å for a_1 and 0.20 Å for a_2 along the molecular short axis. The large slipping distance for a_1 results in the formation of a large cavity where the ReO_4^- ions are situated.

Figure 9. (a) Crystal structure of **5** viewed along the a axis; (b) Columnar structure of MeDTES in **5**; (c) Top view and side view of molecular overlaps of a_1 and a_2 . The atoms in the front molecule are represented by solid circles and those in the rear are represented by open circles.

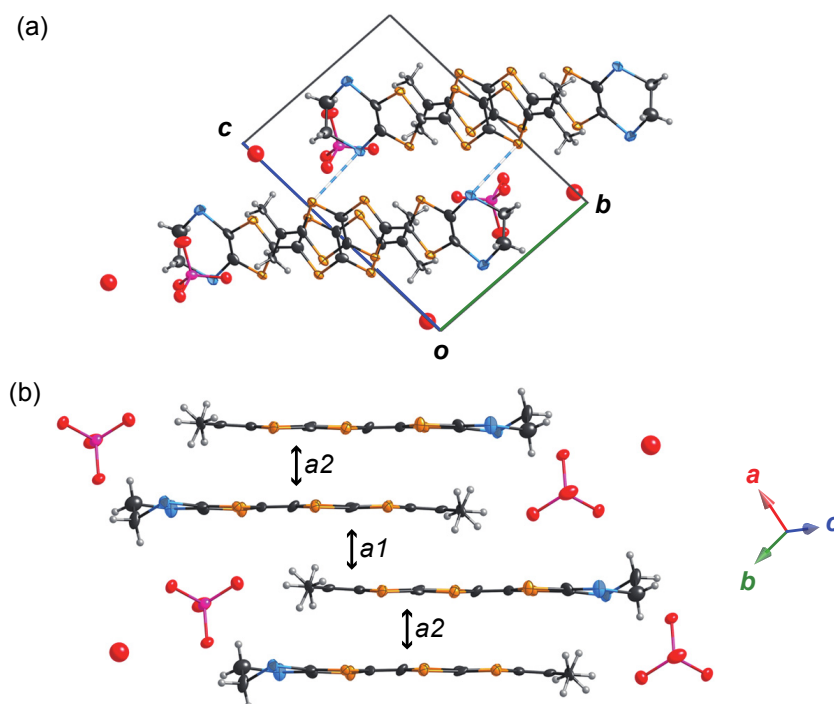
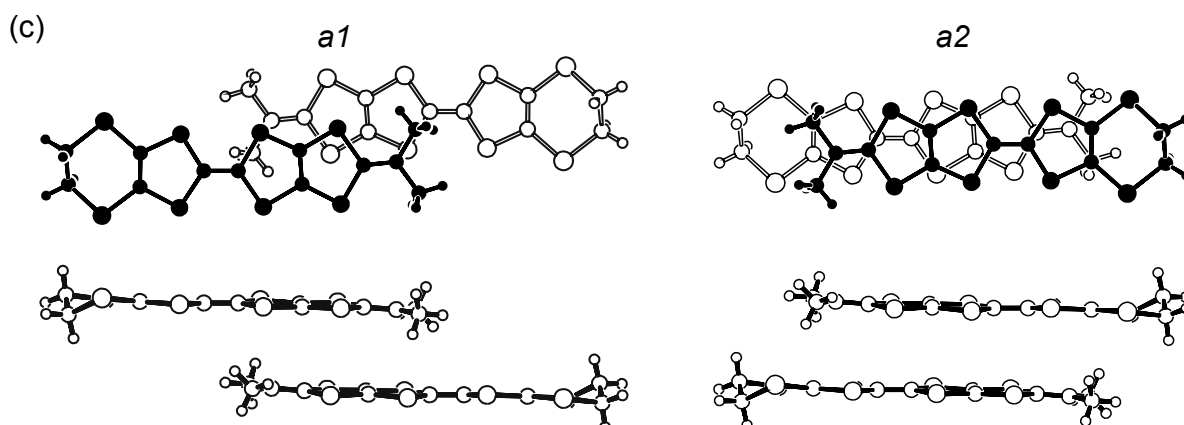


Figure 9. Cont.



The calculated overlap integral $a1$ (-2.04×10^{-3}) is much smaller than the integral $a2$ (21.47×10^{-3}), indicating strong dimerization along the stacking direction (Figure 10). Interestingly, there is a large overlap integral $q2$ because of the existence of short $\text{Se} \cdots \text{S}$ contacts. The energy band structure and Fermi surface were calculated by the tight-binding approximation [23]. There are two energy branches and there is no energy gap between upper and lower bands (Figure 11). If the origin of oxygen atom is an oxonium ion, the Fermi level (E_F) crosses the upper branch, which results in the quasi-one-dimensional metal (Figure 12a). However, the σ_{rt} of the salt is $1.3 \times 10^{-2} \text{ S cm}^{-1}$ and this salt shows semiconducting behavior with small activation energy of 0.058 eV. When the composition of **5** is $(\text{MeDTES})^+(\text{ReO}_4)^-(\text{H}_2\text{O})_{0.5}$, the E_F crosses just through the degeneracy point, which suggest that the salt possesses Fermi points at the B and X points (Figure 12b). The conducting property supports the idea that the origin of oxygen is water and the composition of the salt **5** is $(\text{MeDTES})(\text{ReO}_4)(\text{H}_2\text{O})_{0.5}$.

Figure 10. Molecular arrangement viewed along the molecular long axis. The calculated overlap integrals ($\times 10^{-3}$) are $a1 = -2.04$, $a2 = 21.47$, $p = 0.05$, $q1 = 0.80$, and $q2 = 22.04$. The hydrogen atoms are omitted for clarity.

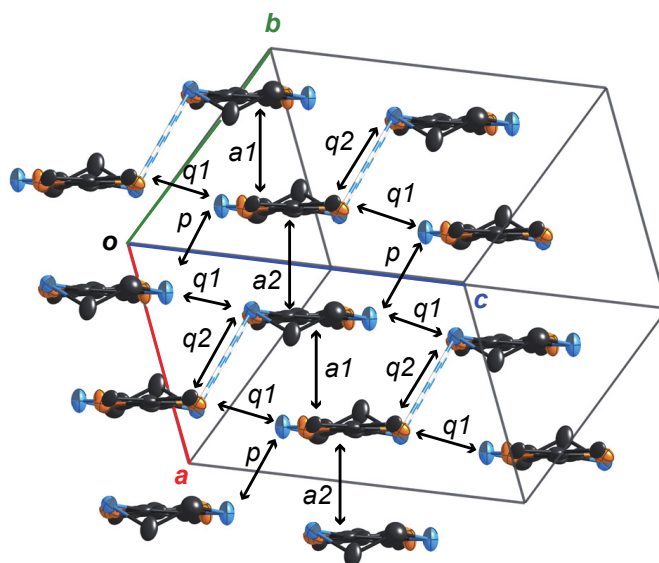


Figure 11. Calculated band dispersion of the salt **5**. The E_F depends on the composition.

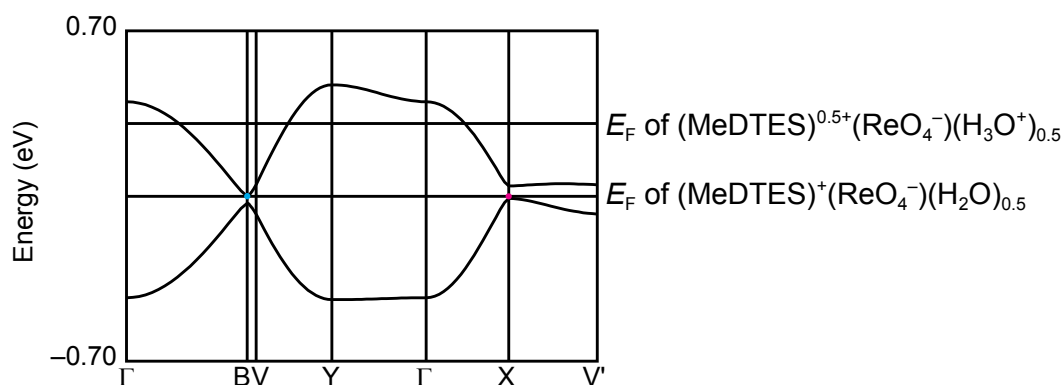
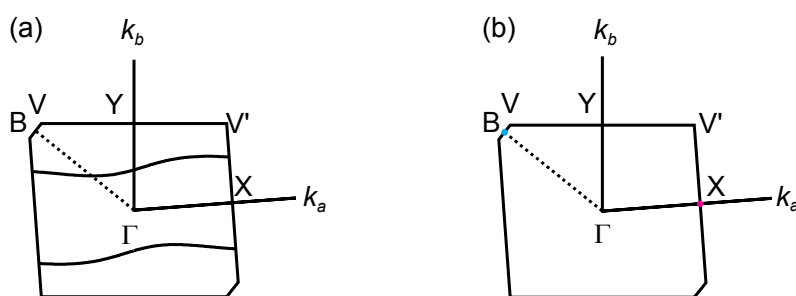


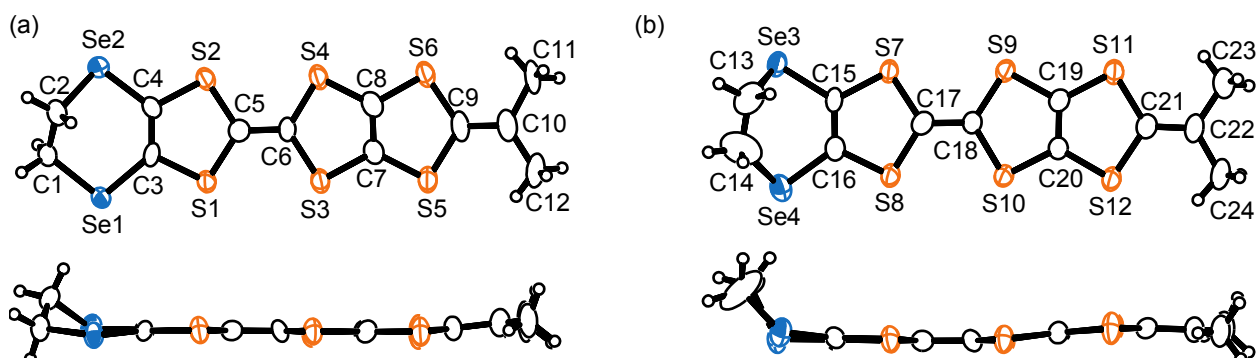
Figure 12. (a) Calculated Fermi surfaces of the composition of $(\text{MeDTES})^{0.5+}(\text{ReO}_4^-)(\text{H}_3\text{O}^+)_{0.5}$. (b) Calculated Fermi points of the composition of $(\text{MeDTES})^+(\text{ReO}_4^-)(\text{H}_2\text{O})_{0.5}$.



2.2.4. Structures and Electrical Properties of $(\text{MeDTES})(\text{I}_3)(\text{DCE})_{0.25}$ (**6**) (DCE = 1,2-Dichloroethane)

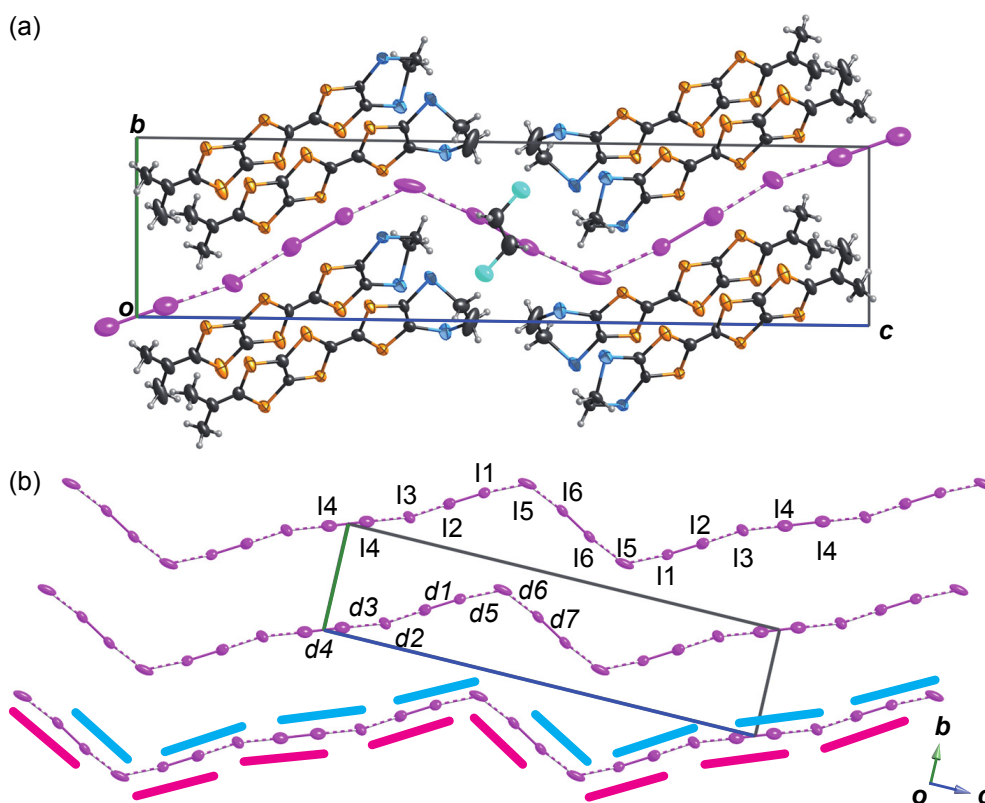
The MeDTES salt with I_3^- (**6**) crystallizes in triclinic space group $P\bar{1}$. There are crystallographically independent two MeDTES molecules. The ORTEP drawings of Molecules A and B of MeDTES are shown in Figure 13. TTF moiety of Molecule A shows high planarity, and the 2-isopropylidene-1,3-dithiole unit slightly bends with dihedral angle of $6.3(3)^\circ$. Molecule B also has flat chair-like structure with dihedral angles $5.9(1)$ and $7.3(3)^\circ$ as shown in Figure 13b.

Figure 13. Top view and side view of ORTEP drawings of (a) Molecule A and (b) Molecule B of MeDTES in **6**. Displacement ellipsoids are drawn at the 50% probability level.



As shown in Figure 14, there is 1,2-dichloroethane (DCE) solvent molecule at around the center of inversion with a half occupancy. Six iodine atoms I1–I6 are crystallographically independent and they form infinite zig-zag chains. The interatomic distances $d1$ (I1–I2), $d4$ (I4–I4), and $d7$ (I6–I6) are 2.900(2), 2.950(2), and 2.935(2) Å, respectively, which are consistent with the average distance of the I–I bond (2.92 Å) in triiodide I_3^- [24,25]. In contrast, the distances $d2$ (I2–I3), $d3$ (I3–I4), $d5$ (I5–I1), and $d6$ (I6–I5) are 3.271(2)–3.471(3) Å which is close to the mean value (3.44 Å) of the I–I bond length of triiodide (2.92 Å) and the sum of the van der Waals radii of iodine atoms (3.96 Å) [21]. The triiodide often forms an infinite chain and the typical $I\cdots I$ distance is 3.60 Å [24], which is slightly longer than $d2$, $d3$, $d5$, and $d6$ of the salt **6**. There might be two patterns of configuration model of triiodide ions which are depicted in Figure 14b as light blue and pink lines. The infinite zig-zag iodine chains observed in the salt **6** are disordered.

Figure 14. (a) Crystal structure of **6** viewed along the a axis; (b) Iodine chain structure in **6** with the atom numberings. Interatomic distances are $d1 = 2.900(2)$, $d2 = 3.271(2)$, $d3 = 3.352(2)$, $d4 = 2.950(2)$, $d5 = 3.471(3)$, $d6 = 3.445(3)$, and $d7 = 2.935(2)$ Å. Two patterns of configuration model of I_3^- ion are depicted as light blue and pink lines.



As shown in Figure 15, Molecules A and B form the head-to-head dimer with an interplanar distance of 3.40 Å and a slipping distance of 0.76 Å along the molecular long axis [5]. The intradimer overlap integral a (-41.80×10^{-3}) is larger than those of the interdimer p (-14.10×10^{-3}) and q (-11.27×10^{-3}). The calculated energy band structure is shown in Figure 16. There are two branches, which are separated by a gap because of the dimerized structure. When the infinite iodide chain consists of polyiodide, such as pentaiodide I_5^- , the Fermi level (E_F) crosses the upper branch, which makes the salt metallic. However, this salt behaves as a semiconductor with an activation energy of

0.051 eV and shows low conductivity $\sigma_{\text{rt}} = 5.3 \times 10^{-2} \text{ S cm}^{-1}$ at room temperature. When the composition of **6** is $(\text{MeDTES})^+(\text{I}_3^-)(\text{DCE})_{0.25}$, the E_{F} lies at the gap (Figure 17), which suggests that the salt **6** is a band insulator. Conductivity measurement supports the idea that the composition of the salt **6** is $(\text{MeDTES})(\text{I}_3)(\text{DCE})_{0.25}$.

Figure 15. (a) Top view and side view of molecular overlap of *a*. The atoms in the front molecule are represented by solid circles and those in the rear are represented by open circles; (b) Molecular arrangement viewed along the molecular long axis. The calculated overlap integrals ($\times 10^{-3}$) are $a = -41.80$, $p = -14.10$, and $q = -11.27$. The infinite iodine chains are depicted by pink circles. The hydrogen atoms are omitted for clarity.

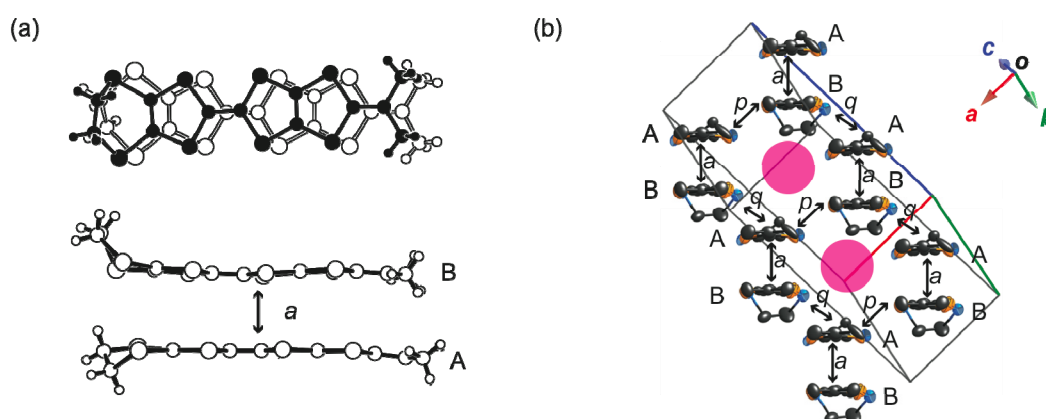


Figure 16. Calculated band dispersion (left) and Fermi surfaces (right) of $(\text{MeDTES})^{3/5+}(\text{I}_5^-)_{3/5}(\text{DCE})_{0.25}$.

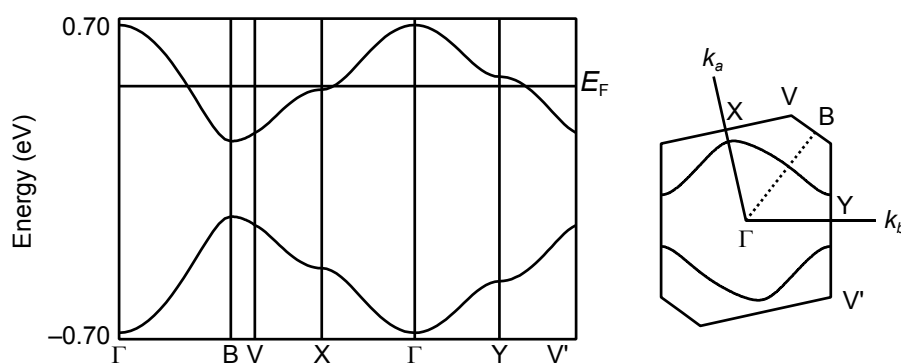
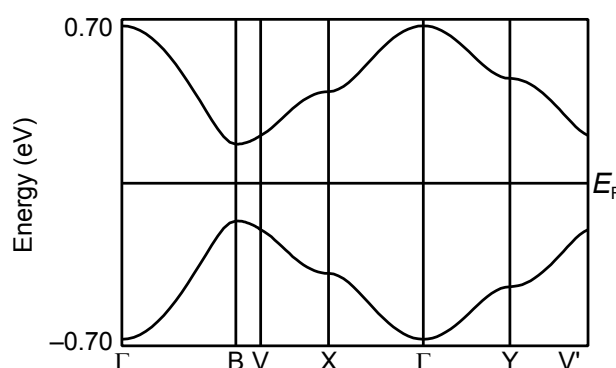


Figure 17. Calculated band dispersion of $(\text{MeDTES})^+(\text{I}_3^-)(\text{DCE})_{0.25}$.



2.2.5. Structures and Electrical Properties of (CPDTES)(I₃) (7)

(CPDTES)(I₃) (7) crystallizes in triclinic space group $P\bar{1}$. The ORTEP drawings of the CPDTES molecule are shown in Figure 18. The molecule takes a flat chair-like structure and the dihedral angles of the TTP moiety composed of the S3–S6 and C6–C9 atoms are 5.7(1) and 6.9(2)°. One donor molecule is crystallographically independent. There are two types of I₃[−] ion in the crystal and two halves of the ions are also crystallographically independent (Figure 19).

Figure 18. Top view (left) and side view (right) of ORTEP drawings for the CPDTES molecule in 7. Displacement ellipsoids are drawn at the 50% probability level.

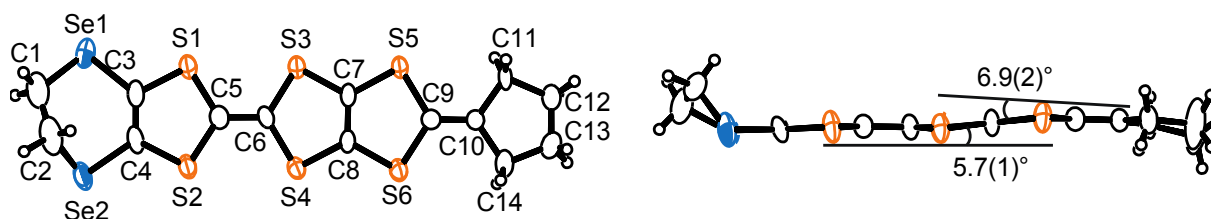
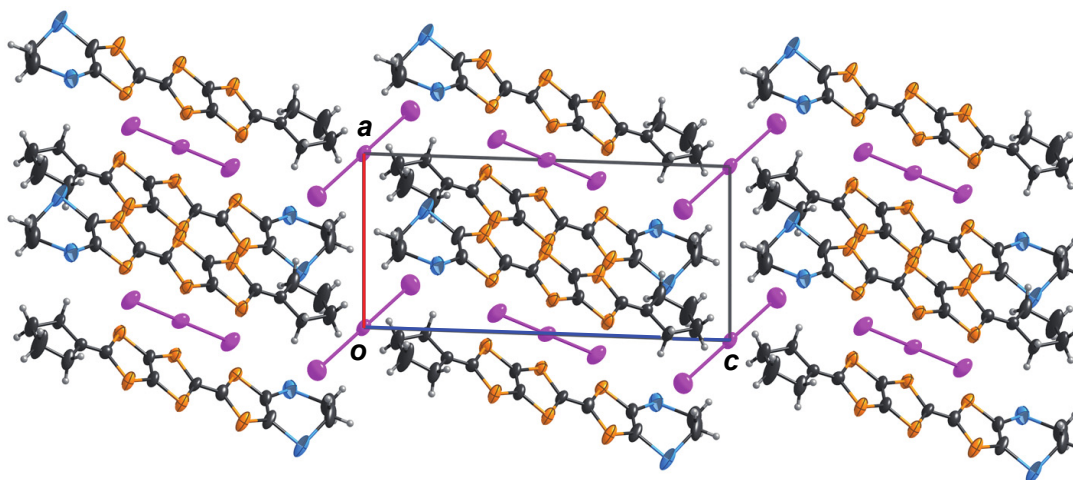


Figure 19. Crystal structure of 7 viewed along the *b* axis.



As shown in Figure 20, donor molecules form a head-to-tail dimer with an interplanar distance of 3.36 Å and a slipping distance of 0.98 Å along the molecular long axis [5]. The dimers are connected by short S⋯S contacts (3.555(3) and 3.583(4) Å) that are shorter than the sum of the van der Waals radii and form a two-dimensional S⋯S network on the *ab* plane. One of the I₃[−] ions is situated in a space surrounded by the donor dimers in the S⋯S network on the *ab* plane. The other I₃[−] ion is situated between the dimers along the *c* axis. Although the S⋯S contacts are formed between the dimers, the interdimer overlap integrals *p* (3.98×10^{-3}) and *q* (7.08×10^{-3}) are much smaller than the intradimer integral *a* (38.11×10^{-3}). Calculated energy band structure reveals that this salt is a band insulator (Figure 21). This result is consistent with the low conductivity ($\sigma_{\text{rt}} = 6.1 \times 10^{-4} \text{ S cm}^{-1}$) and large activation energy ($E_a = 0.17 \text{ eV}$) of the salt.

Figure 20. (a) Top and side views of molecular overlap of a . The atoms in the front molecule are represented by solid circles and those in the rear are represented by open circles; (b) Molecular arrangement viewed along the molecular long axis. The calculated overlaps integrals ($\times 10^{-3}$) are $a = 38.11$, $p = 3.98$, and $q = 7.08$. Orange broken lines and pink circles indicate S...S contacts shorter than the sum of the van der Waals radii and I_3^- ion. The hydrogen atoms are omitted for clarity.

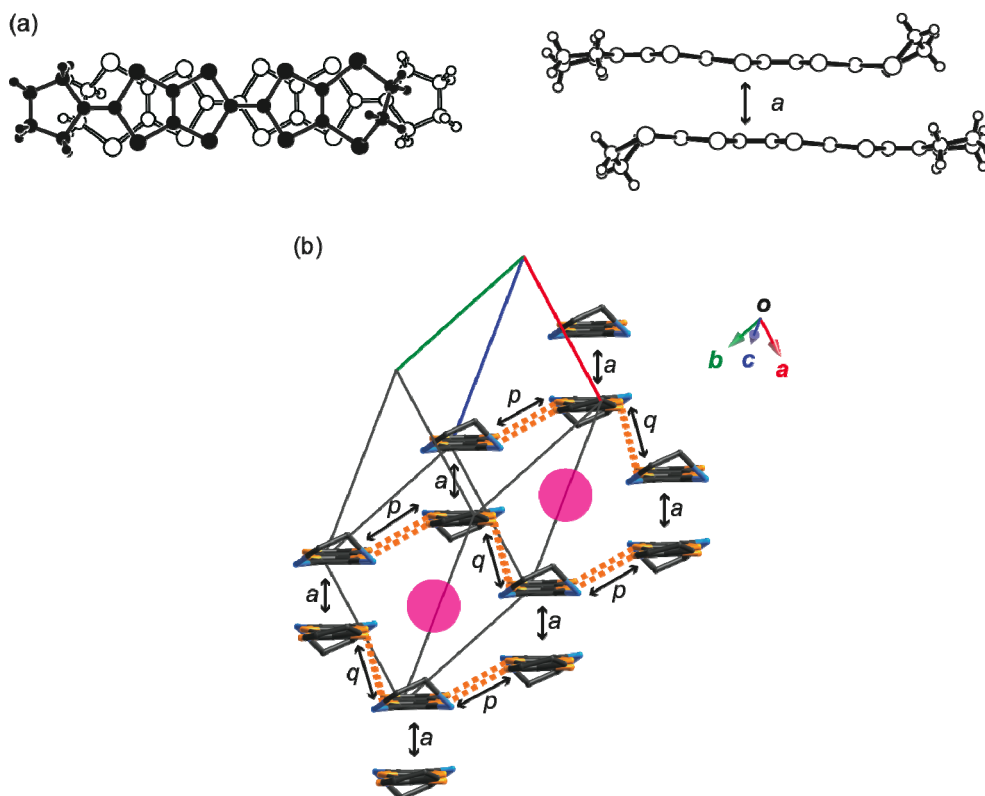
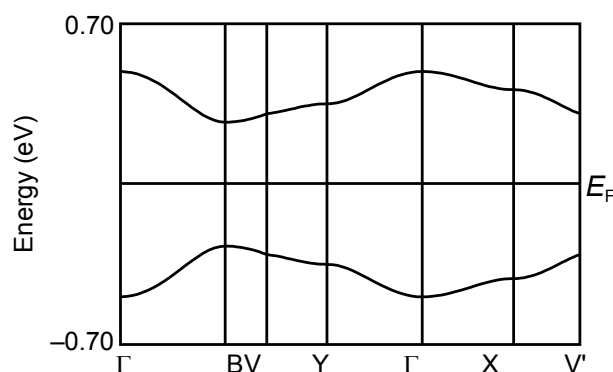


Figure 21. Calculated energy band dispersion of 7.



3. Experimental Section

3.1. General

All chemicals and solvents are of reagent grade. All reactions were conducted under an argon atmosphere. Dehydrated THF was purchased from Wako Pure Chemical Industries, Ltd., and used without further purification. A THF solution of LDA was prepared from diisopropylamine with an

n-hexane solution of *n*-BuLi (1.6 M, Wako Pure Chemical Industries) prior to use. Column chromatography was carried out with silica gel (Kanto Chemical, 100–210 μm and Wakosil[®], 64–210 μm). ¹H NMR spectra were recorded on a JEOL JNM-EX270 spectrometer. The chemical shifts are given in δ (ppm), downfield from internal tetramethylsilane. Mass spectra were measured on Applied Biosystem MALDI-TOF-MS Voyager-DE[™] PRO. The melting points were determined with a Yanaco MP-J3. IR spectra were recorded on a JASCO FT/IR-460 plus spectrometer. Elemental analyses were performed at the Integrated Center for Science, Ehime University. Cyclic voltammetry (CV) measurements were performed using a BAS ALS/chi 617B electrochemical analyzer. The cell for CV consisted of a Pt disk working electrode, a Pt wire counter electrode, and an Ag/AgNO₃ reference electrode. The measurements were carried out in benzonitrile containing 0.1 M tetra-*n*-butylammonium hexafluorophosphate as a supporting electrolyte. All redox potentials were converted relative to a ferrocene/ferrocenium (Fc/Fc⁺) couple. All computations were performed with the Gaussian 09 program package [26] using the 6-31G(d) basis set [27]. Density functional theory (DFT) calculations were carried out using a hybrid method of Hartree-Fock and B3LYP method [28–30].

3.2. Synthesis

3.2.1. Diethyl (5-(5,6-dihydro-[1,4]diselenino[2,3-*d*][1,3]dithiol-2-ylidene)-[1,3]dithiolo[4,5-*d*][1,3]dithiol-2-yl)phosphonate (**3**)

Triethyl phosphite (26 mL) was added to a mixture of 4,5-ethylenediseleno-1,3-dithiole-2-thione (**1**) [17] (1.00 g, 3.14 mmol) and diethyl (5-*oxo*-1,3-dithiolo[4,5-*d*]-1,3-dithiol-2-yl)phosphonate (**2**) [18] (737 mg, 2.23 mmol) in toluene (26 mL), and the solution was stirred at 110 °C for 2 h under argon atmosphere. After cooling to room temperature, the solution was evaporated under reduced pressure to eliminate the solvent and excess of triethyl phosphite. The residue was subjected to silica-gel column chromatography (SiO₂/dichloromethane:ethyl acetate = 10:1). The target compound **3** was isolated as an orange solid (828 mg, 1.38 mmol, 62%). mp 132–136 °C; ¹H NMR (CDCl₃, 270 MHz) δ_{H} 1.37 (t, $J = 6.8$ Hz, 6H), 3.35 (m, 4H), 4.26 (m, 4H), 5.35 (m, 1H); IR (KBr) ν 2979, 2895, 1256, 1162, 1044, 1016, 954, 794, 764, 543, 532 cm⁻¹; LDI-TOF-MS Calcd. for C₁₃H₁₅O₃PS₆Se₂: 601.74 (M⁺). Found: 602.01 with an isotropic pattern of these selenium atoms; Anal. Calcd. for C₁₃H₁₅O₃PS₆Se₂: C, 26.00; H, 2.52%. Found: C, 25.77; H, 2.60%.

3.2.2. 2-Isopropylidene-1,3-Dithiolo[4,5-*d*]-4,5-ethylenediselenotetrathiafulvalene (MeDTES)

A THF solution of LDA (0.5 M, 0.30 mL, 0.15 mmol) was added to a mixture of **3** (65 mg, 0.11 mmol) and acetone (0.10 mL, 1.4 mmol) in dehydrated THF (5 mL) at –78 °C. The reaction mixture was stirred for 2 h at –78 °C, then quenched by addition of methanol (10 mL) and warmed to room temperature. The resulting precipitate was collected by filtration and washed with methanol. The crude product of MeDTES was purified by silica gel column chromatography (SiO₂/carbon disulfide). Analytically pure MeDTES was isolated as orange plates (48 mg, 0.095 mmol, 86%). mp 222–225 °C (decomp.); ¹H NMR (CS₂-C₆D₆, 270 MHz) δ_{H} 1.60 (s, 6H), 3.11 (s, 4H); IR (KBr) ν 2925, 2900, 1433, 1399, 1365, 1266, 963, 766 cm⁻¹; LDI-TOF-MS Calcd. for C₁₂H₁₀S₆Se₂: 505.74 (M⁺). Found: 506.24

with an isotropic pattern of these selenium atoms; Anal. Calcd. for $C_{12}H_{10}S_6Se_2$: C, 28.57; H, 2.00%. Found: C, 28.34; H, 2.26%.

3.2.3. 2-(Pentan-3-ylidene)-1,3-dithiolo[4,5-*d*]-4,5-ethylenediselenotetrathiafulvalene (EtDTES)

A THF solution of LDA (0.5 M, 1.05 mL, 0.53 mmol) was added to a mixture of **3** (247 mg, 0.41 mmol) and 3-pentanone (0.10 mL, 0.94 mmol) in dehydrated THF (15 mL) at -78 °C. The reaction mixture was stirred for 2 h at -78 °C, then quenched by addition of methanol (20 mL) and warmed to room temperature. The same procedure as for MeDTES was adopted for the separation of the products. EtDTES was isolated as orange solid (159 mg, 0.30 mmol, 73%). mp 208–210 °C (decomp.); 1H NMR ($CS_2-C_6D_6$, 270 MHz) δ_H 0.97 (t, $J = 7.8$ Hz, 6H), 2.00 (q, $J = 7.8$ Hz, 4H), 3.10 (s, 4H); IR (KBr) ν 2963, 2925, 1265, 765 cm^{-1} ; LDI-TOF-MS Calcd. for $C_{12}H_{10}S_6Se_2$: 533.78 (M^+). Found: 534.23 with an isotropic pattern of these selenium atoms; Anal. Calcd. for $C_{14}H_{14}S_6Se_2$: C, 31.57; H, 2.65%. Found: C, 31.43; H, 2.70%.

3.2.4. 2-Cyclopentanylidene-1,3-dithiolo[4,5-*d*]-4,5-ethylenediselenotetrathiafulvalene (CPDTES)

A THF solution of LDA (0.5 M, 0.30 mL, 0.15 mmol) was added to a mixture of **3** (67 mg, 0.11 mmol) and cyclopentanone (0.10 mL, 1.12 mmol) in dehydrated THF (5 mL) at -78 °C. The reaction mixture was stirred for 2 h at -78 °C, then quenched by addition of methanol (20 mL) and warmed to room temperature. The same procedure as for MeDTES was adopted for the separation of the products. EtDTES was isolated as orange solid (40 mg, 0.075 mmol, 68%). mp 198–201 °C (decomp.); 1H NMR ($CS_2-C_6D_6$, 270 MHz) δ_H 1.25 (m, 4H), 1.75 (m, 4H), 3.22 (s, 4H); IR (KBr) ν 2938, 2906, 2869, 1620, 1516, 1425, 1266, 766 cm^{-1} ; LDI-TOF-MS Calcd. for $C_{14}H_{12}S_6Se_2$: 531.76 (M^+). Found: 532.23 with an isotropic pattern of these selenium atoms; Anal. Calcd. for $C_{12}H_{10}S_6Se_2$: C, 28.57; H, 2.00%. Found: C, 28.34; H, 2.26%.

3.3. Preparation of Cation Radical Salts

Single crystals of the cation radical salts of MeDTES and CPDTES were prepared by the galvanostatic oxidation under the conditions listed in Table 2. Platinum wire electrodes (2.0 mm ϕ) and standard H-shaped cells were employed.

3.4. X-Ray Crystallographic Analysis

The diffraction data were collected on a Rigaku Saturn724 diffractometer using multi-layer mirror monochromated Mo- K_α radiation ($\lambda = 0.71075$ Å) at the Integrated Center for Science, Ehime University. The structures were solved by the direct method (SIR2004 [31], SIR2008 [32], and SHELXS-97 [33]). All calculations were performed using the CrystalStructure crystallographic software package [34] except for full-matrix least squares refinement on F^2 , which was performed using SHELXL-97 [33]. Crystal data collection and refinement parameters for (MeDTES)[Au(CN) $_4$] (**4**), (MeDTES)(ReO $_4$)(H $_2$ O) $_{0.5}$ (**5**), (MeDTES)(I $_3$)(DCE) $_{0.25}$ (**6**), and (CPDTES)(I $_3$) (**7**) are summarized in Table 3. CCDC-879812, CCDC-879813, CCDC-879814, and CCDC-879815 (for **4**, **5**, **6**, and **7**)

contain the supplementary crystallographic data for this paper. These data can be obtained free of charge from the Cambridge Crystallographic Data Centre via www.ccdc.cam.ac.uk/data_request/cif.

3.5. Band Calculations

From the results of the X-ray crystal structure analysis, intermolecular overlap integrals were calculated using highest occupied molecular orbitals (HOMOs) of the donor molecules obtained by the extended Hückel MO calculations. The electronic band dispersions and Fermi surfaces were calculated using the intermolecular transfer integrals under the tight-binding approximation [23].

3.6. Electrical Resistivity Measurement

Electrical resistivities were measured by the four-probe method using YOKOGAWA 7651 programmable direct current source and KEITHLEY 2001 digital multimeter unit. Gold wires (10 μm φ diameter) were attached to a single crystal using carbon paste. The sample was cooled using an Iwatani CryoMini model CRT-HE05-RE cooling system and the temperature was controlled using Lakeshore S331 digital program temperature controller. Electrical properties of **4–7** are summarized in Table 3.

4. Conclusions

A series of DT-TTF derivatives containing ethylenediseleno group have been synthesized, and crystal structures, band structures, and electrical properties of their cation radical salts have been investigated. There is no distinct difference in the electrochemical properties between the ethylenediseleno-substituted donors and the ethylenedithio-substituted donors. In contrast, crystal structures of the cation radical salts are different. It is known that the ethylenedithio-substituted DT-TTFs tend to afford the κ -type molecular conductors with non-half-filled bands [10,11], and the self-aggregating property is the key to form the κ -type molecular arrangement [35]. The self-aggregating property is associated with the moderate steric hindrance of the ethylenedithio group. The theoretical calculation of MeDTES reveals that the replacement of sulfur atoms in the ethylenedithio group by larger selenium atoms leads to an enhancement of steric hindrance. As a result, the self-aggregating property has disappeared in the present ethylenediseleno-containing donor system, and MeDTES and CPDTES yielded cation radical salts with various crystal structures. The dimerized structure is observed in the salts **5–7** and the donor-anion ratio of the salts is 1:1. Calculated energy bands of these salts consist of two branches. Their conductivity results support the idea that the E_F lies in the gap and crosses just through the degeneracy point. If cation radical salts with a 2:1 donor-anion ratio could be obtained, the E_F might cross the upper branch, which is in favor of formation of effective half-filling conductors. At the moment, we have obtained a small size $\text{Au}(\text{CN})_2^-$ salt of MeDTES with poor quality and preliminary structure analysis suggests the β -type donor arrangement with the 2:1 donor-anion ratio. This salt could be a candidate for the new organic metals including organic superconductors. Preparation of high quality single crystals of such cation radical salts is underway.

Acknowledgments

This work is partially supported by Grant-in-Aid for Scientific Research (Nos. 15073215, 19740202, 20110006, 21750148, and 23550155) from the Ministry of Education, Culture, Sports, Science and Technology, Japan, and Japan Society for the Promotion of Science, and by Grant-in-Aid for Research Promotion from Ehime University, and Advanced Low Carbon Technology Research and Development Program (ALCA) of Japan Science and Technology Agency (JST).

References

1. Ishiguro, T.; Yamaji, K.; Saito, G. *Organic Superconductors*, 2nd ed.; Cardona, M., Fulde, P., von Klitzing, K., Queisser, H.-J., Eds.; Springer-Verlag: Berlin, Germany, 1998.
2. Williams, J.M.; Thorn, R.J.; Ferraro, J.R.; Carlson, K.D.; Geiser, U.; Wang, H.H.; Kini, A.M.; Whangbo, M.-H. *Organic Superconductors (Including Fullerenes) Synthesis, Structure, Properties, and Theory*; Grimes, R.N., Ed.; Prentice-Hall: Upper Saddle River, NJ, USA, 1992.
3. Urayama, H.; Yamochi, H.; Saito, G.; Nozawa, K.; Sugano, T.; Kinoshita, M.; Sato, S.; Oshima, K.; Kawamoto, A.; Tanaka, J. A new ambient pressure organic superconductor based on BEDT-TTF with T_c higher than 10 K ($T_c = 10.4$ K). *Chem. Lett.* **1988**, *17*, 55–58.
4. Williams, J.M.; Kini, A.M.; Wang, H.H.; Carlson, K.D.; Geiser, U.; Montgomery, L.K.; Pyrka, G.J.; Watkins, D.M.; Kammers, J.M. From semiconductor-semiconductor transition (42 K) to the highest- T_c organic superconductor, κ -(ET)₂Cu[N(CN)₂]Cl ($T_c = 12.5$ K). *Inorg. Chem.* **1990**, *29*, 3272–3274.
5. Mori, T. Structural genealogy of BEDT-TTF-based organic conductors I. Parallel Molecules: β and β' Phases. *Bull. Chem. Soc. Jpn.* **1998**, *71*, 2509–2526.
6. Mori, T. Structural genealogy of BEDT-TTF-based organic conductors II. Inclined molecules: θ , α , and κ phases. *Bull. Chem. Soc. Jpn.* **1999**, *72*, 179–197.
7. Aonuma, S.; Okano, Y.; Sawa, H.; Kato, R.; Kobayashi, H. Stable molecular metals based on a novel unsymmetrical diselenadithiafulvalene. *J. Chem. Soc. Chem. Commun.* **1992**, *1992*, 1193–1195.
8. Misaki, Y.; Nishikawa, H.; Fujiwara, H.; Kawakami, K.; Yamabe, T.; Yamochi, H.; Saito, G. (2-Methylidene-1,3-dithiolo[4,5-*d*])tetrathiafulvalene (DT-TTF): New unsymmetrical TTFs condensed with 1,3-dithiol-2-ylidene moieties. *J. Chem. Soc. Chem. Commun.* **1992**, *1992*, 1408–1409.
9. Misaki, Y.; Taniguchi, M.; Miura, T.; Fujiwara, H.; Yamabe, T.; Kawamoto, T.; Mori, T. Structures and properties of MeDTDM salts. *Adv. Mater.* **1997**, *9*, 663–635.
10. Misaki, Y.; Nishikawa, H.; Yamabe, T.; Mori, T.; Inokuchi, H.; Mori, H.; Tanaka, S. Structure and Electrical Properties of MeDTET Salts. *Chem. Lett.* **1993**, *22*, 1341–1344.
11. Fujiwara, H.; Misaki, Y.; Taniguchi, M.; Yamabe, T.; Kawamoto, T.; Mori, T.; Mori, H.; Tanaka, S. Preparation, structures and physical properties of κ -type two-dimensional conductors based on unsymmetrical extended tetrathiafulvalene: 2-cyclopentanylidene-1,3-dithiolo[4,5-*d*]-4,5-ethylenedithiotetrathiafulvalene (CPDTET). *J. Mater. Chem.* **1998**, *8*, 1711–1717.
12. Takimiya, K.; Otsubo, T. Selenium-containing π -conjugated compounds for electronic molecular materials. *Phosphorus Sulfur Silicon Relat. Elem.* **2005**, *180*, 873–881.

13. Otsubo, T.; Takimiya, K. Selenium Analogues of TTFs. In *TTF Chemistry—Fundamentals and Applications of Tetrathiafulvalene: Selenium Analogues of TTFs*; Yamada, J., Sugimoto, T., Eds.; Kodansha & Springer: Tokyo, Japan, 2004; Chapter 5, pp. 119–136.
14. Imakubo, T.; Shirahata, T.; Kibune, M.; Yoshino, H. Hybrid organic/inorganic supramolecular conductors $D_2[Au(CN)_4]$ [$D =$ diiodo(ethylenedichalcogeno)tetrachalcogenofulvalene], including a new ambient pressure superconductor. *Eur. J. Inorg. Chem.* **2007**, *2007*, 4727–4735.
15. Wang, H.H.; Montgomery, L.K.; Geiser, U.; Porter, L.C.; Carlson, K.D.; Ferraro, J.R.; Williams, J.M.; Cariss, C.S.; Rubinstein, R.L.; Whitworth, J.R.; *et al.* Syntheses, structures, selected physical properties and band electronic structures of the *bis*(ethylenediseleno) tetrathiafulvalene salts, $(BEDSe-TTF)_2X$, $X^- = I_3^-$, AuI_2^- , and IBr_2^- . *Chem. Mater.* **1989**, *1*, 140–148.
16. Sakata, J.; Sato, H.; Miyazaki, A.; Enoki, T.; Okano, Y.; Kato, R. Superconductivity in new organic conductor κ -(BEDSe-TTF) $_2$ CuN(CN) $_2$ Br. *Solid State Commun.* **1999**, *108*, 377–381.
17. Garín, J.; Orduna, J.; Savirón, M.; Bryce, M.R.; Moore, A.J.; Morisson, V. Synthesis and characterization of functionalized ethylenediselenotetrathiafulvalenes: A comparative study with their all-sulfur analogues. *Tetrahedron* **1996**, *52*, 11063–11074.
18. Masaki, Y.; Ohta, T.; Higuchi, N.; Fujiwara, H.; Yamabe, T.; Mori, T.; Mori, H.; Tanaka, S. A vinyllog of *bis*-fused tetrathiafulvalene: Novel π -electron framework for two-dimensional organic metals. *J. Mater. Chem.* **1995**, *5*, 1571–1579.
19. Takahashi, K.; Tanioka, H.; Fueno, H.; Masaki, Y.; Tanaka, K. Preparation and characterization of novel aromatic-inserted tris-fused tetrathiafulvalenes. *Chem. Lett.* **2002**, *31*, 1002–1003.
20. Imakubo, T.; Shirahata, T.; Kibune, M. Synthesis, crystal structure and electrochemical properties of *bis*(ethylenedioxy)tetraselenafulvalene (BEDO-TSeF). *Chem. Commun.* **2004**, *2004*, 1590–1591.
21. Bondi, A. van der Waals volumes and radii. *J. Phys. Chem.* **1964**, *68*, 441–451.
22. Kistenmacher, T.J.; Phillips, T.E.; Cowan, D.O. The crystal structure of the 1:1 radical cation-radical anion salt of 2,2'-*bis*-1,3-dithiole (TTF) and 7,7,8,8-tetracyanoquinodimethane (TCNQ). *Acta Cryst.* **1974**, *B30*, 763–768.
23. Mori, T.; Kobayashi, A.; Sasaki, Y.; Kobayashi, H.; Saito, G.; Inokuchi, H. The intermolecular interaction of tetrathiafulvalene and *bis*(ethylenedithio)tetrathiafulvalene in organic metals. Calculation of orbital overlaps and models of energy-band structures. *Bull. Chem. Soc. Jpn.* **1984**, *57*, 627–633.
24. Svensson, P.H.; Kloo, L. Synthesis, structure, and bonding in polyiodide and metal iodide-iodine systems. *Chem. Rev.* **2003**, *103*, 1649–1684.
25. Mizuno, M.; Tanaka, J.; Harada, I. Electronic spectra and structures of polyiodide chain complexes. *J. Phys. Chem.* **1981**, *85*, 1789–1794.
26. Frisch, M.J.; Trucks, G.W.; Schlegel, H.B.; Scuseria, G.E.; Robb, M.A.; Cheeseman, J.R.; Scalmani, G.; Barone, V.; Mennucci, B.; Petersson, G.A.; *et al.* *Gaussian 09*, Revision C.01; Gaussian, Inc.: Wallingford, CT, USA, 2010.
27. Hehre, W.J.; Ditchfield, R.; Pople, J.A. Self-consistent molecular orbital methods. XII. Further extensions of Gaussian—Type basis sets for use in molecular orbital studies of organic molecules. *J. Chem. Phys.* **1972**, *56*, 2257–2261.

28. Becke, A.D. Density-functional exchange-energy approximation with correct asymptotic behavior. *Phys. Rev. A* **1988**, *38*, 3098–3100.
29. Becke, A.D. Density-functional thermochemistry. III. The role of exact exchange. *J. Chem. Phys.* **1993**, *98*, 5648–5652.
30. Lee, C.; Yang, W.; Parr, R.G. Development of the Colle-Salvetti correlation-energy formula into a functional of the electron density. *Phys. Rev. B* **1998**, *37*, 785–789.
31. Burla, M.C.; Caliandro, R.; Camalli, M.; Carrozzini, B.; Cascarano, G.L.; Caro, L.D.; Giacovazzo, C.; Polidori, G.; Spagna, R. *SIR2004*: An improved tool for crystal structure determination and refinement. *J. Appl. Cryst.* **2005**, *38*, 381–388.
32. Burla, M.C.; Caliandro, R.; Camalli, M.; Carrozzini, B.; Cascarano, G.L.; de Caro, L.; Giacovazzo, C.; Polidori, G.; Siliqi, D.; Spagna, R. *IL MILIONE*: A suite of computer programs for crystal structure solution of proteins. *J. Appl. Cryst.* **2007**, *40*, 609–613.
33. Sheldrick, G.M. A short history of *SHELX*. *Acta Cryst.* **2008**, *A64*, 112–122.
34. Rigaku, M. *CrystalStructure*, Version 4.0; Rigaku Corporation: Tokyo, Japan, 2010.
35. Misaki, Y. Tetrathiapentalene-based organic conductors. *Sci. Technol. Adv. Mater.* **2009**, *10*, 024301:1–024301:22.

© 2012 by the authors; licensee MDPI, Basel, Switzerland. This article is an open access article distributed under the terms and conditions of the Creative Commons Attribution license (<http://creativecommons.org/licenses/by/3.0/>).